Environmental Science Nano

ROYAL SOCIETY OF CHEMISTRY

PAPER

Cite this: *Environ. Sci.: Nano*, 2022, **9**, 2440

Fe_3O_4 nanoparticles affect paddy soil microbial-driven carbon and nitrogen processes: roles of surface coating and soil types†

Jiangbing Xu,[a] Yaqian Chen,[a] Jingyi Luo,[a] Jiatong Xu,[a] Guoyi Zhou,[a] Yingliang Yu,[b] Lihong Xue,[b] Linzhang Yang[b] and Shiying He *[b]

Received 22nd December 2021,
Accepted 15th May 2022

DOI: 10.1039/d1en01177d

rsc.li/es-nano

Magnetic Fe_3O_4 nanoparticles (nFe_3O_4) are the most widely used nanomaterials and are inevitably introduced to soils. To overcome particle agglomeration, nFe_3O_4 are often coated with protective agents. However, scarce information has addressed the impacts of surface coating of nFe_3O_4 on biochemical processes and microbial properties in soil. In this study, a laboratory incubation experiment was employed to reveal the response of gas production, mineral N content, enzymatic activities and soil bacterial community to nFe_3O_4 and *meso*-2,3-dimercaptosuccinic acid coated nFe_3O_4 (nFe_3O_4@DMSA) in three representative paddy soils in China, *i.e.* lateritic soil (LS), Wushan soil (WS), and red soil (RS). The results showed that nFe_3O_4@DMSA, rather than nFe_3O_4, influenced these parameters profoundly, with varying effects in the soil types. Specifically, in RS nFe_3O_4@DMSA, rather than nFe_3O_4, promoted the CH_4 production, soil NH_4-N concentration, and soil enzymatic activities of β-xylanase (BX) and β-*N*-acetylglucosaminidase (NAG), but decreased the CO_2 production and β-glucosidase (BG) activity. By contrast, in LS and WS nFe_3O_4@DMSA led to increases in CO_2 emission, soil NH_4-N content, and BG, BX, and NAG activities, but a decrease in CH_4 production. Data from 16S rRNA gene sequencing showed the varying responses to the nanoparticles in terms of soil bacterial taxa and putative functional groups. The methanogens and the N-fixation group had strong affinities with the CH_4 production and NH_4-N content, respectively. *Geobacter* was closely related to the CH_4 production in all soils. *Anaeromyxobacter*, *Azospirillum*, and *Burkholderia–Caballeronia–Paraburkholderia* had close relationships with the N-fixation group/NH_4-N content in LS, WS and RS, respectively. Collectively, nFe_3O_4@DMSA changed the microbial-driven biochemical process in the soils, depending on the soil types. Caution should be paid to the complex interaction between the soil matrix and nanoparticle types for better management of nanoparticles in future.

Environmental significance

Our findings provided a fundamental understanding of the role of nFe_3O_4@DMSA in soil biochemical processes. nFe_3O_4@DMSA led to more profound changes in gas production, mineral N content, enzymatic activities and soil bacterial community compared to nFe_3O_4, and such effects of nFe_3O_4@DMSA varied with soil types. This is the first study to compare the effects of coated and uncoated nFe_3O_4 on the microbial-driven C and N processes in soil. Such information sheds light on the nanoparticle management in agricultural ecosystems.

Introduction

Recent advances in materials science and nanotechnology have allowed nanoparticles (<100 nm) to be widely used in various fields.[1,2] Magnetite Fe_3O_4 nanoparticles (nFe_3O_4), whose counterpart Fe_3O_4 macroparticles are ubiquitously distributed in the environment,[3–5] have attracted tremendous attention owing to their excellent physical and chemical properties, *e.g.* high conductivity, high surface area, high biocompatibility, and easy modification on their surface.[6,7] In recent years, increasing use of nFe_3O_4 for crop protection

[a] *Institute of Ecology, Jiangsu Key Laboratory of Agricultural Meteorology, School of Applied Meteorology, Nanjing University of Information Science and Technology, Nanjing 210044, China*
[b] *Institute of Agricultural Resources and Environment, Jiangsu Academy of Agricultural Sciences, No. 50, Zhongling Street, Nanjing 210014, China. E-mail: hshiying@hotmail.com; Tel: +86 025 84391526*

† Electronic supplementary information (ESI) available. See DOI: https://doi.org/10.1039/d1en01177d

and fertilization in agriculture has been observed.[8,9] Moreover, the use of nFe_3O_4 is promising for soil pollution remediation, because they show apparent capacity to trap and remove toxic metal ions, and then they can be easily separated under external magnetic fields.[10] As such, increasing release of nFe_3O_4 into the environment is expected.

Accordingly, concerns have been raised about the fate and behavior of nanoparticles and their biological impacts on organisms in the environment.[11] Soil microorganisms are the active components in soil and are sensitive to environmental perturbations. The incorporation of nanoparticles affects the micro-niches for microorganisms and the subsequent biochemical process in soil. For example, Kamran *et al.*[12] found that nFe_3O_4 are toxic to microbes and suppress N mineralization in soil. Zhang *et al.*[13] reported that nFe_3O_4 increase the population of microbial taxa associated with C cycling, such as *Nocardia*, *Chitinophaga sancti*, *Rhizobium* and *Burkholderia–Paraburkholderia*, but decrease the N fixation related bacteria *Bradyrhizobiaceae* and iron-redox bacteria *Sediminibacterium*. It was also found that nFe_3O_4 enhance soil enzymatic activities (*i.e.* cellulase and dehydrogenase), microbial growth,[9] and the relative abundance of some CH_4-producing microorganisms.[14] Our previous studies[15,16] have demonstrated that nFe_3O_4 stimulate bacterial growth, alter the soil bacterial community and potentially change the C and N cycling in agricultural soils.

To improve their colloidal stability or biocompatibility, nanoparticles are often coated with functional groups.[17] Many materials, such as proteins, polymers, chitosan, polyrhodanine or other organic molecules, are considered to be good alternatives for surface modification of iron oxide nanoparticles (IONPs), but their impacts on organisms varied to different extents.[10,18] Buchman *et al.*[19] reported that a mesoporous silica coating reduces dissolution of IONPs, thus mitigating their impact on *Shewanella oneidensis*. That is because the coating can control the dissolution of the IONP core by reducing the amount of released iron ions, making IONPs a more sustainable option to reduce perturbations to the ecosystem upon release of nanoparticles into the environment. Recently, *meso*-2,3-dimercaptosuccinic acid (DMSA, surface-bound sulfur-containing molecules) has been preferred as a coating material due to its good chelating capability with metals and its harmlessness to humans or other mammals.[20] Previous studies have studied the stability of DMSA-coated nFe_3O_4 (nFe_3O_4@DMSA) and their impact on aquatic organisms,[20–22] but whether nFe_3O_4@DMSA would influence terrestrial organisms has not been explored yet.

In terrestrial ecosystems, soil properties vary a lot in the aspects of soil texture, pH, soil organic matter (SOM), metal oxides, *etc.*, which subsequently affect the dispersity and bio-availability of nanoparticles in soil. For instance, soil pH may influence the mobility of nFe_3O_4.[9] SOM could adsorb readily onto nanoparticles, significantly enhancing the suspension stability of nanoparticles.[23,24] In view of these, we hypothesized that the coated nanoparticles would have more marked impacts on the microbial-induced biochemical process (C and N cycling) than the uncoated ones in soil, and such effects varied with soil types. To this end, a laboratory incubation experiment was employed by adding nFe_3O_4 and nFe_3O_4@DMSA to three representative paddy soils collected from subtropical areas of China. The CH_4 and CO_2 production, soil enzymatic activities and the bacterial community structure were determined across the incubation period. The objectives of this study were to: i) assess the extents to which the above parameters responded to nFe_3O_4 and nFe_3O_4@DMSA in different soils and ii) reveal the representative bacteria responsible for the biochemical changes in soils. The results will provide a perspective on the microbial response to the surface modified nFe_3O_4 nanoparticles and a comprehensive understanding of environmental implications of nanoparticles.

Materials and methods

Preparation of nanoparticles

Two different Fe_3O_4 nanoparticles used in this study were synthesized by a co-precipitation method. Briefly, $FeCl_3{\cdot}6H_2O$ and $FeSO_4{\cdot}7H_2O$ solutions (molar ratio 2 : 1) were mixed under vigorous stirring and nitrogen gas protection. Then $NH_3{\cdot}H_2O$ was added dropwise into the above mixture and kept at 50 °C. The resulting solution turned black in color after 2 h, indicating the formation of nFe_3O_4. The nFe_3O_4 were filtered and washed three times with distilled water by magnetic separation. The obtained nFe_3O_4 were finally vacuum dried overnight. The nFe_3O_4@DMSA were prepared by mixing 0.5 g DMSA and 250 mL of Fe_3O_4 solution (the mass ratio between DMSA and the nanoparticles was 1 : 2) and then the mixture was stirred vigorously for 3 h at 50 °C. Subsequently, Fe_3O_4@DMSA were obtained by alternately washing the nanoparticles with ethanol and DI water to remove the residual DMSA. Transmission electron microscopy (TEM, Tecnai 12, Philips, The Netherlands) was used to determine the morphology and sizes of the synthesized nanoparticles (Fig. 1). The zeta potentials and hydrodynamic size distributions (PSD) of the particles were measured using a zeta potential analyzer (Zetasizer Nano Zs90, Malvern Instruments Ltd, UK).

Soil sampling and soil property testing

Three typical paddy soils used in this study were collected from the southern parts of China. Lateritic soil (LS, Anthrosol, 0–20 cm depth) was collected from Xiayuan Village of Huishan City (23°08′N, 114°64′E), Guangdong Province, China. Red soil (RS, Udic Ferrosols, 0–20 cm depth) was collected from Yingtan City (28°15′N, 116°55′E), Jiangxi Province, China. Wushan soil (WS, Anthrosol, 0–20 cm) was collected from Suzhou City (31°7′N, 120°30′E), Jiangsu Province, China. These soils had a neutral to acidic pH, but represented a wide range of paddy soils in subtropical regions of China.

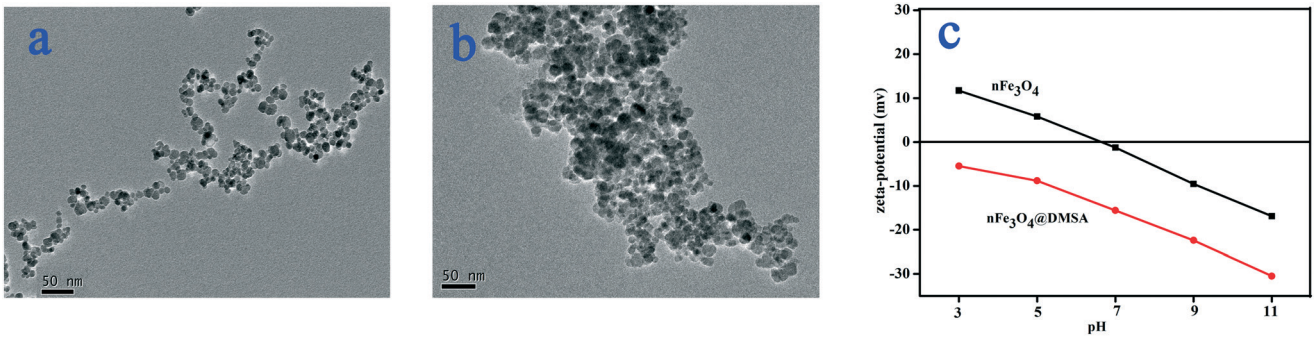

Fig. 1 TEM images showing synthesized nFe_3O_4. (a) nFe_3O_4@DMSA; (b) uncoated nFe_3O_4. The zeta potential of the two nanoparticles (c).

Table 1 Physicochemical properties of the soils used for the incubation experiment

	pH	SOM mg g^{-1}	TN	TP	TK	Total_Fe	Bio-Fe mg kg^{-1}	C/N
LS	5.68b	24.70b	1.21b	0.64a	17.1a	16.14a	23.47b	11.93
WS	6.32a	41.33a	1.62a	0.48b	9.27b	9.72b	22.38b	14.97
RS	5.01c	30.85b	1.43b	0.52ab	4.40c	8.51b	32.13a	12.80

SOM: soil organic matter, TP: total phosphate, TN: total nitrogen, TK: total potassium, Bio-Fe: bioavailable Fe. LS, WS and RS represent lateritic soil (Guangdong, China), Wushan soil (Jiangsu, China), and red soil (Jiangxi, China), respectively. Different letters in the same column indicate significant differences between soils collected from different sites.

After collection, the soil samples were air-dried and crushed to pass through a 60 mesh screen for further use. The physicochemical characteristics of the three soils were determined according to standard methods.[25] The bioavailable Fe in soil was estimated with the 0.01 mol L^{-1} $CaCl_2$ method, followed by atomic absorption spectrophotometry (FAAS, flame AAS). The properties are summarized in Table 1.

Incubation experiment

For each soil, a batch of 110 ml serum bottles was prepared. Each bottle was filled with 5 mg glucose, 10 g soil and 15 ml deionized water. The bottles were capped with rubber stoppers and incubated and waterlogged in the dark at 25 °C for a week to activate microbial activity. At the end of pre-incubation, 4 mg urea, 4 mg dipotassium phosphate and 1 mg of the following nanoparticles were added into each bottle. Three treatments were set up for each soil: (1) control: soil with no nanoparticles, (2) nFe_3O_4 treatment: soil with nFe_3O_4 added, and (3) nFe_3O_4@DMSA treatment: soil with nFe_3O_4@DMSA added. To clarify the dynamics of the biochemical process, each treatment was performed in triplicate for each sampling time, *i.e.* days 7, 14, 28 and 56. Then, the serum bottles were capped with butyl. The top gas was substituted with pure N_2 to ensure anaerobic conditions. Finally, the soils were incubated at 25 °C in the dark. At days 1, 3, 7, 12, 17, 25, 35, 47, and 54, the gaseous samples were collected for determining the CH_4 and CO_2 concentrations. At days 7, 14, 28 and 56, three replicates for each treatment were taken for soil biochemical determination and soil DNA extraction.

CH_4 and CO_2 production

On each sampling day, a 10 ml gaseous sample was collected from the headspace of each serum bottle using a syringe. The concentrations of CH_4 and CO_2 in the gaseous sample were analyzed using a gas chromatograph GC-7890A (Agilent Technologies, Palo Alto, CA, United States) equipped with a flame ionization detector.

Mineral N content in soil

On each sampling day, the soil was extracted with 2 M KCl by shaking at 150 rpm for 60 min at 22 °C. Extracts were filtered using a 90 mm (diameter) Whatman No. 41 ashless filter paper (Fisher Scientific) under vacuum and were subsequently stored at −20 °C until analysis. The extracts were analyzed for ammonium and nitrate (NO_3 and NO_2) levels using a Skalar San++ flow analyzer (Skalar Inc., Breda, The Netherlands) as per the manufacturer's instructions.

Soil enzymatic activities

The assays were performed using a fluorescent standard 4-methylumbelliferone (MUB) (Sigma-Aldrich, St. Louis, MO, USA) and fluorescently-labelled substrates, *i.e.* 4-methylumbelliferyl-phosphate, 4-methylumbelliferyl-β-D-glucopyranoside, 4-methylumbelliferyl-β-D-xylopyranoside, and 4-methylumbelliferyl *N*-acetyl-β-D-glucosaminide (Sigma-

Aldrich, St. Louis, MO, USA) for acidic phosphatase (AP), β-glucosidase (BG), β-xylanase (BX) and β-*N*-acetylglucosaminidase (NAG), respectively. Briefly, 1 g of the test soil (dry weight) was suspended in 100 mL of sterile deionized water in triplicate and was homogenized using a rotary shaker at 180 rpm. Two hundred microliters of the resultant soil homogenate was added to each well of a black 96-well plate (Costar 3916, VWR International) followed by the buffer, substrate and standard. The plates were incubated at 20 °C in the dark for 2 h and read at 365 nm excitation and 460 nm emission on a Synergy H1 multi-well spectrofluorometer (Biotek, Winooski, VT, USA).

Soil DNA extraction, PCR amplification and processing of high throughput sequencing data

Soil total genomic DNA was extracted using a FastDNA® SPIN kit for soil (MP Biomedicals, Santa Ana, CA), according to the manufacturer's instructions. The extracted DNA was dissolved in 50 μl TE buffer, quantified by gel electrophoresis and evaluated using a NanoDrop™ One (Thermo Fisher, Waltham, MA, USA), and then stored at −20 °C until further use.

PCR was carried out with the primer pair 515F (5′-GTGC CAGCMGCCGCGGTAA-3′) and 806R (5′-GGAC TACHVGGGTWTCTAAT-3′) targeting the V4 region of the bacterial 16S rRNA gene.[26] The 5 bp barcoded oligonucleotides were fused to the forward primer. Each PCR 50 μl reaction mixture contained 1.25 μM deoxynucleoside triphosphate, 2 μl (15 μM) of forward and reverse primers, 2 μM Taq DNA polymerase (TaKaRa, Japan), and 1 μl (50 ng) of genomic DNA as a template. Each reaction was performed in triplicate to balance the bias in the amplification process. The negative control was always run with sterile water as the template instead of the soil DNA extract. Amplifications were carried out using the thermal conditions as follows: 94 °C for 5 min, 30 cycles (94 °C for 30 s, 55 °C for 30 s, and 72 °C for 45 s), and a final extension at 72 °C for 10 min. The reaction products for each sample were pooled and purified using a QIAquick® PCR purification kit (Qiagen, Germantown, MD, USA) and quantified using a NanoDrop™ One (Thermo Fisher, Waltham, MA, USA).

High throughput sequencing data were analyzed using the Quantitative Insight into Microbial Ecology (QIIME) 1.9.0 pipeline (**https://www.qiime.org**). Sequences with lengths <200 bp were discarded, and chimaeras were filtered with UPARSE. Operational taxonomic units were delineated using a 97% similarity threshold, and taxonomy was determined using Silva 132 (**https://www.arb-silva.de**) for the bacterial community. FAPROTAX infers the microbial community profile into a putative functional profile.[27] Raw sequences were submitted to the NCBI Sequence Read Archive (SRA) under SRA accession number PRJNA783514.

Statistical analysis

For statistical processing we used R.[28] One-way analysis of variance (ANOVA) with *post hoc* Tukey's honest significant difference (HSD) test was used to compare the differences among the treatments. *P*-Values < 0.05 were taken as significant. The relationships between the functional groups of bacterial community and the biochemical properties of soil were analyzed by redundancy analysis (RDA) and envfit analysis in R using the "vegan" library (permutation = 999). The Pearson correlation coefficient was calculated by a cor() function and visualized by using the corrplot package, and the significance level was tested by the cor.mtest() function in the R environment.

Results

Characteristics of nFe_3O_4 and nFe_3O_4@DMSA

Surface charge and size distribution play important roles in determining nanoparticle behavior in soil systems. As shown in Fig. 1, the sizes of nFe_3O_4 and nFe_3O_4@DMSA were about 10–20 nm, while the hydrodynamic diameter was decreased from 233.6 nm to 53.8 nm after coating with DMSA. The surface charge of nFe_3O_4@DMSA was negative in the pH range from 3.0–11.0, while nFe_3O_4 was positive at pH lower than 7.0 and negative at higher pH.

CH_4 and CO_2 production

The CH_4 production displayed a lag for all soils, but the lag phases differed in the soils (Fig. 2). It took about 7 days of lag phase for WS and RS before the onset of rapid CH_4 production, while a longer lag (24 d) was observed in LS, implying the low methanogenic process in LS.

For the different nanoparticles, nFe_3O_4@DMSA had a more profound impact than nFe_3O_4 on CH_4 production, but the effects differed with the soil types. Specifically, nFe_3O_4@DMSA inhibited the CH_4 production, being significant after day 25 and day 12 for LS and WS, respectively ($P < 0.05$). In contrast, in RS nFe_3O_4@DMSA enhanced the CH_4 production significantly compared to the control after day 12 ($P < 0.05$). Similarly, remarkable changes were detected for nFe_3O_4@DMSA in terms of CO_2 production in all soils, rather than for nFe_3O_4. In LS and WS, higher CO_2 productions were achieved by nFe_3O_4@DMSA than by the control, being significant after day 17 ($P < 0.05$). However, in RS a statistically significant decrease of CO_2 production was detected for nFe_3O_4@DMSA after day 25 ($P < 0.05$).

Soil mineral N content

The nanoparticles changed the mineral N content in all soils to different extents in comparison with the control, with sound changes observed in nFe_3O_4@DMSA, rather than in nFe_3O_4 (Fig. 3). In LS, nFe_3O_4@DMSA had the potential to decrease the NH_4-N content, with a significantly lower value than the control at day 14 and day 28 ($P < 0.05$). In WS, nFe_3O_4@DMSA had a significantly higher NH_4-N content than both the control and nFe_3O_4 at day 7 and day 14 ($P < 0.05$); the NO_3-N content was significantly higher in nFe_3O_4@DMSA than in the other treatments at day 14 ($P < 0.05$). In RS, a

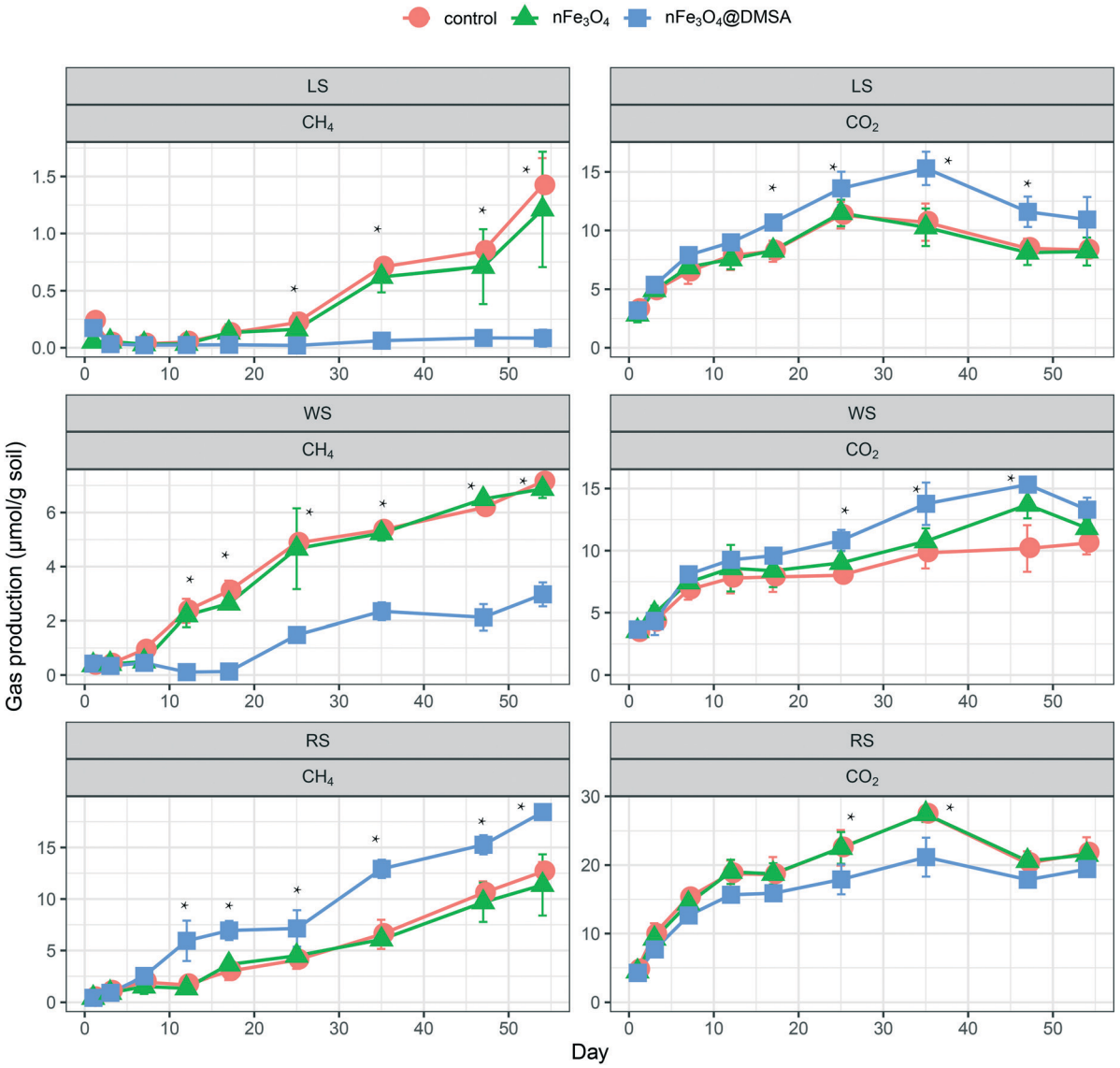

Fig. 2 CH_4 and CO_2 productions from different soils with and without nanoparticles. Control, without nanoparticle addition; nFe_3O_4, soil treated with nFe_3O_4; nFe_3O_4@DMSA, soil treated with nFe_3O_4@DMSA. LS, WS and RS represent lateritic soil (Guangdong, China), Wushan soil (Jiangsu, China), and red soil (Jiangxi, China), respectively. * indicates the significant difference among different treatments at the corresponding time of incubation.

significantly higher NH_4-N content was found in nFe_3O_4@DMSA than in both the control and nFe_3O_4 at day 7 ($P < 0.05$).

Soil enzymatic activities

The potential activities of the four enzymes (AP, BG, BX, and NAG) responded to the nanoparticles to different extents (Fig. 4). AP did not show significant changes among all treatments across soils, while the other enzymatic activities varied with the soil types and nanoparticles. Specifically, compared to the control, nFe_3O_4@DMSA, rather than nFe_3O_4, increased values of BG and NAG in LS, being significant at day 28. In WS, nFe_3O_4@DMSA had higher values of BG, BX and NAG than the control, being significant for most of the time of incubation. In RS, BX and NAG were stimulated by nFe_3O_4@DMSA, with significantly higher values than those for the control at day 28 ($P < 0.05$). Note that in RS both nFe_3O_4@DMSA and nFe_3O_4 significantly decreased the value of BG at days 7 and 14 in comparison with the control ($P < 0.05$), but had approaching values with the control afterwards (at days 28 and 54). No significant differences in these enzymatic activities were found between nFe_3O_4 and the control in RS ($P < 0.05$).

Soil bacteria lineages related to C and N cycling

Due to the close affinity between the biochemical processes (*i.e.* gas production and enzymatic activities) and the microbial properties, we paid special attention to the

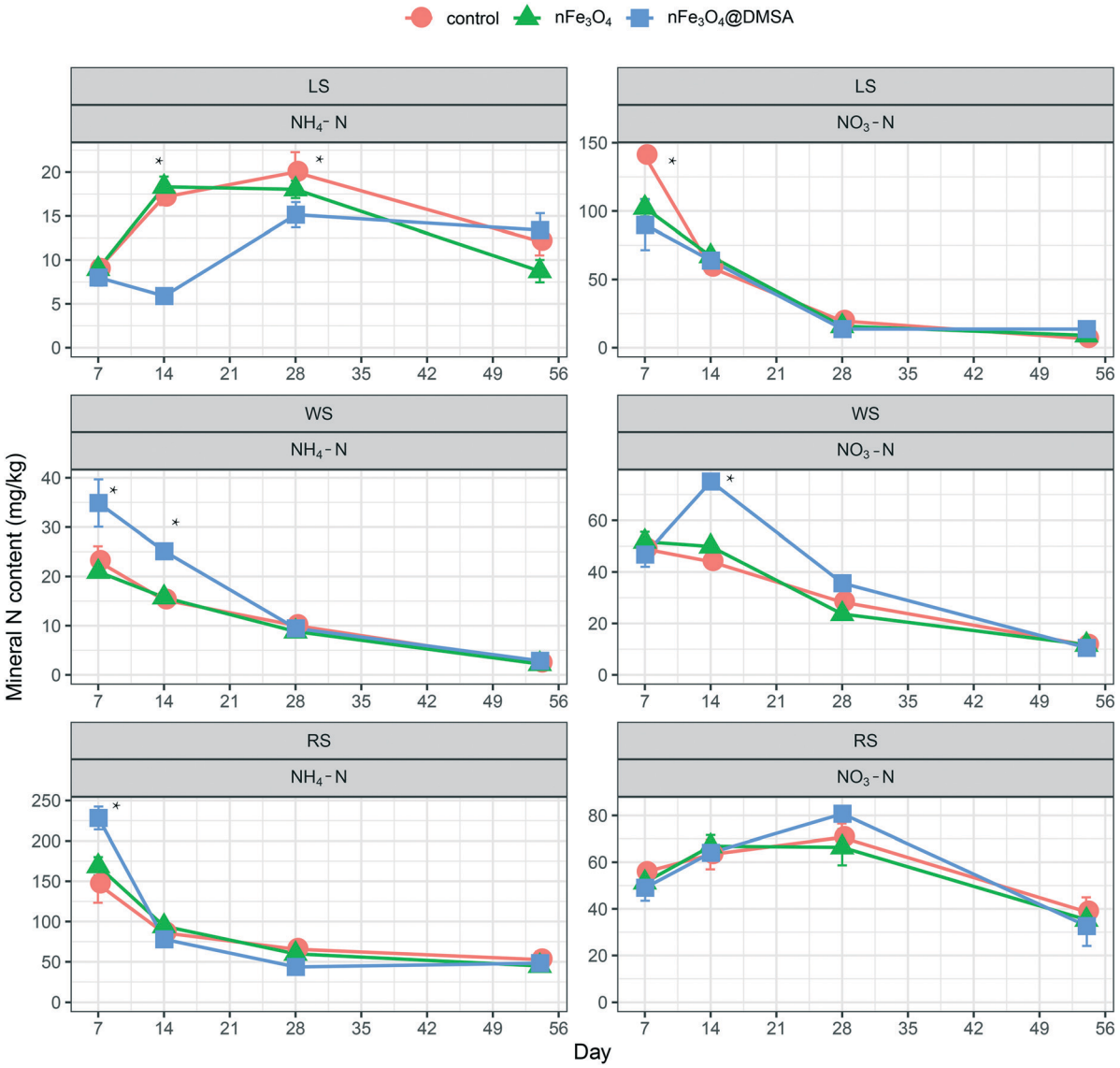

Fig. 3 Mineral N contents (NH_4-N and NO_3-N) in soils across the incubation period. Control, without nanoparticle addition; nFe_3O_4, soil treated with nFe_3O_4; nFe_3O_4@DMSA, soil treated with nFe_3O_4@DMSA. LS, WS and RS represent lateritic soil (Guangdong, China), Wushan soil (Jiangsu, China), and red soil (Jiangxi, China), respectively. * indicates the significant difference among different treatments at the corresponding time of incubation.

representative lineages associated with these processes, *e.g. Geobacter* and *Methanosarcina* for CH_4 production, and *Mesorhizobium*, *Azospirillum*, *Anaeromyxobacter*, *Burkholderia–Caballeronia–Paraburkholderia*, *Hyphomicrobium*, *Leptothrix*, *Skermanella*, *Methylobacterium*, and *Azotobacter* for N fixation. The total and the individual proportions of each group were calculated separately (Fig. 5, S1 and S2†). Different trends were observed between nFe_3O_4@DMSA and nFe_3O_4.

For the taxa associated with CH_4 production, no significant differences were detected for the total abundance among the treatments in all soils (Fig. 5), but distinct responses were found for individual lineages (Fig. S1 and S2†). As compared to the control, both nFe_3O_4@DMSA and nFe_3O_4 significantly decreased the relative abundance of *Geobacter* in both LS ($P < 0.05$ at days 7 and 28) and WS ($P <$ 0.05 at days 14 and 28), but an opposite trend was shown in RS ($P < 0.05$ at day 28). No significant differences were found for *Methanosarcina* and *Methanobacterium* among the treatments across all soils. For the lineages associated with N fixation, nFe_3O_4@DMSA produced an increase in their total abundance in RS ($P < 0.05$ at days 7 and 14, Fig. 5), but had an inhibiting effect in LS ($P < 0.05$, at days 7 and 28). Individually, *Anaeromyxobacter*, *Azospirillum*, and *Hyphomicrobium* in LS had significantly lower proportions in nFe_3O_4@DMSA than in the control at the initial stage of incubation. *Anaeromyxobacter* and *Azospirillum* in WS had higher relative abundances in nFe_3O_4@DMSA than in the control at different periods of incubation, *i.e.* at day 54 for *Anaeromyxobacter*, and days 7 and 28 for *Azospirillum*. In RS, the relative abundances of *Azotobacter*, *Burkholderia–*

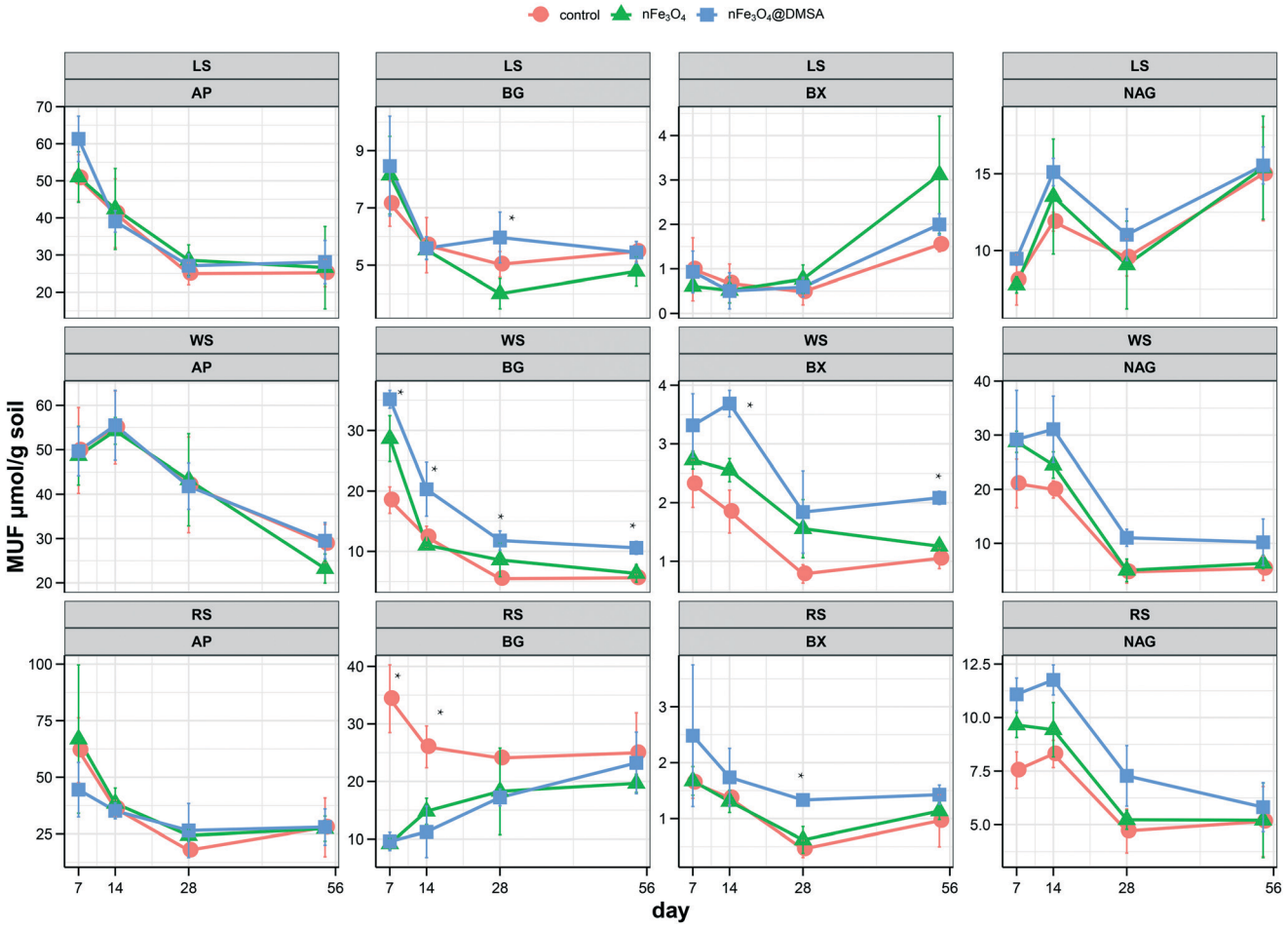

Fig. 4 Enzymatic activities in different soils treated with or without nanoparticles. Control, without nanoparticle addition; nFe_3O_4, soil treated with nFe_3O_4; nFe_3O_4@DMSA, soil treated with nFe_3O_4@DMSA. LS, WS and RS represent lateritic soil (Guangdong, China), Wushan soil (Jiangsu, China), and red soil (Jiangxi, China), respectively. AP, BG, BX and NAG represent the enzymatic activities of acidic phosphatase, β-glucosidase, β-xylanase, and β-*N*-acetylglucosaminidase, respectively. * indicates the significant difference among different treatments at the corresponding time of incubation.

Caballeronia–Paraburkholderia, and *Methylobacterium* had increasing trends led by nFe_3O_4@DMSA compared to the control, with significant differences at day 28 for *Azotobacter*, and at days 7 and 14 for both *Burkholderia–Caballeronia–Paraburkholderia* and *Methylobacterium* ($P < 0.05$).

Relationships between the soil bacterial community and soil biochemical properties

The FAPROTAX database was used to infer the putative functional groups of the bacterial community. Considering the significant changes appearing at the initial period of incubation, we selected the representative time for characterizing the functional bacterial groups, *i.e.* day 14 for LS and WS and day 28 for RS. The proportions of several functional groups showed significant changes in the soils with different nanoparticles (Fig. S3†). In particular, nFe_3O_4@DMSA significantly increased the proportion of the N fixation group in WS and RS, but significantly decreased that in LS ($P < 0.05$).

Further RDA and correlation analyses demonstrated the relationships between the soil biochemical properties and bacterial functional group/taxa (Fig. 6). In LS, nFe_3O_4@DMSA showed positive effects on the nitrate reduction and fermentation groups, which were significantly correlated with CO_2 production, NO_3-N, and NAG (Fig. 6a and d). By contrast, the control in LS positively affected N fixation and nitrification groups, with significant correlations with NH_4-N and CH_4 (Fig. 6a and d). Moreover, significant correlations between *Geobacter* and CH_4, and between *Burkholderia–Caballeronia–Paraburkholderia* and BX were detected in LS ($P < 0.05$).

In WS, positive effects of nFe_3O_4@DMSA were found on the N fixation and iron respiration, which were concurrently positively correlated with BG, BX, NH_4-N and CO_2 production (Fig. 6b and e). In contrast, the control in WS showed a positive impact on methanogenesis, fermentation and CH_4 production. Correlation analysis showed the significantly positive correlations between *Burkholderia–Caballeronia–Paraburkholderia* and BX and BG, and between *Geobacter* and CH_4.

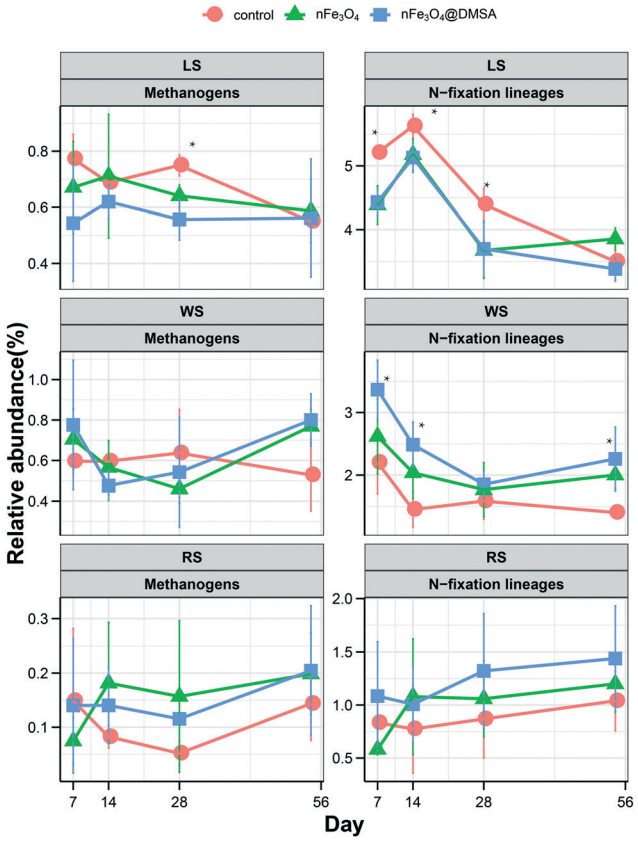

Fig. 5 The total relative abundances of the bacterial lineages of methanogens and N-fixation lineages. Control, without nanoparticle addition; nFe_3O_4, soil treated with nFe_3O_4; nFe_3O_4@DMSA, soil treated with nFe_3O_4@DMSA. LS, WS and RS represent lateritic soil (Guangdong, China), Wushan soil (Jiangsu, China), and red soil (Jiangxi, China), respectively. * indicates the significant difference among different treatments at the corresponding time of incubation.

In RS, a different pattern was found as compared to that in LS or WS. The nFe_3O_4@DMSA led to the enrichment of the methanogenesis group, which had significant correlations with CH_4, BX, and NAG. By contrast, the control had positive effects on the fermentation and hydrocarbon degradation groups (Fig. 6c and f). Correlation analysis showed positive correlations between *Burkholderia–Caballeronia–Paraburkholderia* and NH_4-N, and between *Geobacter* and CH_4.

Discussion

Impacts of nFe_3O_4@DMSA and nFe_3O_4 on gas production

Iron oxides are regarded as important electron acceptors in subtropical soils, and organic C in soils might be anaerobically decomposed to CH_4 and CO_2 following the reduction of iron oxides.[29] Many studies have explored the effect of nFe_3O_4 on CH_4 production, with the results aligning with the trend that nFe_3O_4 stimulate the methanogenesis under the circumstances of anaerobic digestion,[30] wastewater plants,[31,32] and soil ecosystems.[4,11,33] However, this was not the case observed in this study showing the negligible changes in CH_4 production led by nFe_3O_4 across all soils. We assumed that such a discrepancy might be ascribed to the differences in the C supply between our studies and the foregoing studies. In the literature, a trait shared is the existence of a large quantity of organic C (labile C in particular), either from the direct C amendment or in the C-rich environment.[4,30,33,34] In this case, humic acid and fulvic acid are easily formed, and their ligand exchange reactions with the surface of nFe_3O_4 facilitate the proliferation of methanogens, resulting in the accelerated CH_4 production. The importance of organic C for methanogenesis was partially evidenced in this study by the long lag phase together with the low CH_4 production in LS that had a relatively lower SOM content among the tested soils. Besides, the low-C environment also explained the statistical similarities in CH_4 production between nFe_3O_4 and the control in all soils.

Our study further suggested that, not only the supply of organic C, but also the surface characteristics of the nanoparticles and other soil properties played crucial roles in regulating the CH_4 production (Fig. 2). The latter two factors were proposed to explain the patterns observed in the nFe_3O_4@DMSA treatments in the different soils. Specifically, in RS the surface characteristics of nFe_3O_4@DMSA might contribute largely to the enhanced CH_4 production, while in LS and WS the form of Fe species (such as bioavailable Fe^{3+}) in the soils would be greatly associated with the inhibited CH_4 production. Compared with nFe_3O_4, the particles of nFe_3O_4@DMSA possess very active surface sites facilitating their binding with the recalcitrant or complicated C in soil.[12] Fermentation can easily occur by discharging electrons to protons forming H_2 or formate, which could be finally used by syntrophic methanogens.[7,33] It is known that the growth of a typical methanogen *Geobacteraceae* (or *Geobacter*) relies strictly on the presence of iron oxide nanoparticles and their electrical conductivity in particular.[35,36] The addition of iron oxides promoted the electron transfer between *Geobacter* and other methanogens to promote CH_4 production,[37] and the positive correlation between *Geobacter* and CH_4 production has been observed in paddy soils and lake sediments.[3,38] The evidence here was the similar trends of CH_4 production and the proportion of *Geobacter* enhanced by nFe_3O_4@DMSA in RS during the incubation, and their significant correlation at day 14 as well (Fig. 6, S1 and S2†). Besides, *Geobacter* can serve as a sign of the Fe state in soil. The decline of *Geobacter* indicates that the bioavailable Fe^{3+} is completely reduced to Fe^{2+} and could be readily precipitated as $FeCO_3$ (siderite) under anaerobic conditions.[39,40] From this point of view, the relatively lower content of bioavailable Fe ($CaCl_2$ extractable Fe) in LS and WS of this study might play a more important role than the active surface sites of nFe_3O_4@DMSA in influencing the methanogenic process, resulting in the suppressed growth of *Geobacter* and subsequently the lower CH_4 production in the nFe_3O_4@DMSA treatments. However, questions

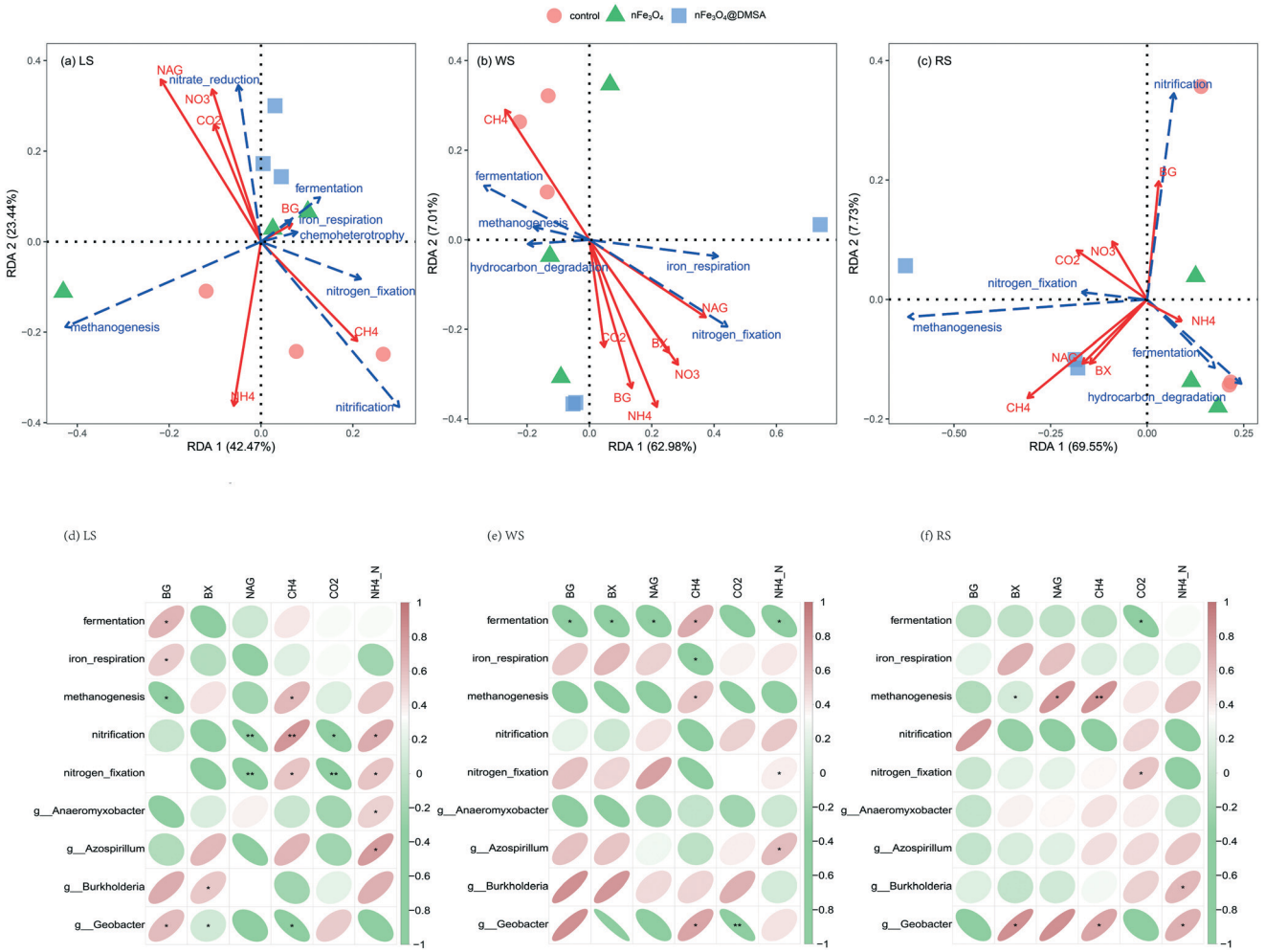

Fig. 6 Redundancy analysis (RDA) of putative functional groups and biochemical properties in LS (a), WS (b) and RS (c). In the RDA plots, the blue dashed arrows indicate the direction of several selected functional groups, and the red solid arrows indicate the direction of several biochemical property changes along the gradients of explanatory variables. The correlation analyses between functional groups (or lineages) and biochemical properties for LS (d), WS (e) and RS (f) are located beneath the RDA plots. * – correlation is significant at $P < 0.05$; ** – correlation is significant at $P < 0.01$. Control, without nanoparticle addition; nFe_3O_4, soil treated with nFe_3O_4; nFe_3O_4@DMSA, soil treated with nFe_3O_4@DMSA. LS, WS and RS represent lateritic soil (Guangdong, China), Wushan soil (Jiangsu, China), and red soil (Jiangxi, China), respectively.

remained why nFe_3O_4 did not inhibit CH_4 production, and how the nFe_3O_4@DMSA interacted with soil bioavailable Fe^{3+} in LS and WS. To answer these questions, perhaps an in-depth investigation is needed from the aspect of Fe species because they are highly associated with hydroxyl radicals and further affect organic matter cycling in soil.[41,42]

For the CO_2 emission, an opposite trend to CH_4 production was observed when subjected to Fe_3O_4@DMSA incorporation (Fig. 2). A plausible explanation is that the total fermentation group might be stimulated when the process of methanogenesis was inhibited under anaerobic conditions, indirectly producing considerable quantities of CO_2 capable of forming siderite with reduced iron.[35,40] This was supported in this study by the negative relationship between CO_2 and CH_4 in the RDA plot across all soils (Fig. 6). Note that CO_2 emission (or microbial respiration from soil) is considered as a direct indicator of microbial activity.[12] The effect of Fe_3O_4 nanoparticles on soil microbial activity has been reported, with results depending on soil types.[8,43]

Impacts of nFe_3O_4@DMSA and nFe_3O_4 on C cycling in soils

Extracellular enzymes play important roles in the ecosystem function of soil, including element cycling and microbial metabolism.[44] They are sensitive to external disturbances and serve as indicators of soil quality. Changes in the activity of extracellular enzymes have been used to demonstrate the effects of nanoparticles on soil functions.[45,46] In this study, the potential of several important extracellular enzymes was selected to signify the C cycling in soil. The principal function of BG is hydrolysis of cellobiose and other β-1,4 glucans to glucose. BX and NAG are analogous to the role of BG in cellulose degradation, but different in degrading the complex components. BX indicates the degradation of xylooligomers (short xylan chains) into xylose.[47] NAG plays a

role in the degradation of chitin and other β-1,4-linked glucosamine polymers.[48]

In the present study, nFe_3O_4@DMSA, rather than nFe_3O_4, accelerated the activities of BG, BX and NAG in both LS and WS, suggesting the superiority of nFe_3O_4@DMSA over nFe_3O_4 in stimulating the C-related cycling, *via* strengthening the decomposition of xylooligomers, cellulose and chitin. This was concurrent with the patterns of CO_2 emission that showed higher microbial activity in nFe_3O_4@DMSA. As elucidated above, the reduction of nanoparticle Fe^{3+} is accompanied by oxidation of SOM. The adsorption of nFe_3O_4@DMSA on SOM can facilitate the electron transfer and the accelerated mobility of SOM, and provide more substrates for hydrolysis.[11] In this sense, the positive relationship here between the fermentation group and the activity of BG or BX (Fig. 6) indicated the enhanced C cycling *via* decomposing the complex C substances in nFe_3O_4@DMSA-added soil. In support, previous studies have shown that nFe_3O_4 improve the BG activity in soil, regardless of whether the surface of the nanoparticles is modified or not.[14,49] An exception was the decreased activity of BG caused by nFe_3O_4@DMSA in RS, albeit the increased activities of BX and NAG. In view of the gas emission patterns, we assumed that the hydrolyzed products (such as cellobiose and other β-1,4 glucans) from xylooligomers and chitin were primarily served as the substrates for methanogens, but less for other microorganisms, resulting in the suppressed BG in RS from the aspect of whole microbial community. As such, diverse metabolic pathways of microorganisms existed in soils after adding nFe_3O_4@DMSA, with various responses in the different soils.

Impacts of nFe_3O_4@DMSA and nFe_3O_4 on N cycling in soils

The mineral N content was used to characterize the bioavailable N in soil. In this study, a soil-dependent pattern was observed in terms of the mineral N content after adding the nanoparticles, implying the complex interaction between the nanoparticles and soil matrix. A minor effect of nFe_3O_4 on the soil bacterial community has been reported,[50] supporting the present results. By contrast, a marked change was observed for the NH_4-N content that was increased by nFe_3O_4@DMSA in WS and RS, but was decreased in LS at day 14. From the physicochemical aspect, it has been suggested that the NH_4-N adsorption–desorption equilibrium in soil is influenced not only by soil pH, clay, redox potential, and SOM,[51] but also by the reduction and dissolution of iron oxides, controlling NH_4-N fixation in flooded paddy soil.[52] Hence, soil properties/types are important factors influencing the N-related cycling in nFe_3O_4@DMSA-added soil. Unfortunately, such chemical processes were not the key points of this study, and we were unable to provide a suitable explanation from this aspect. From the microbial point of view, the putative N fixation group and the typical diazotrophic taxa (Fig. 6) were addressed due to the fact that iron is a cofactor in several enzymes, as a part of cytochromes, and a participant in biochemical reactions including N fixation.[43] The resembling trends between the NH_4-N content and the total relative abundance of selected diazotrophic taxa signified the important role of diazotrophs in N-cycling in this study (Fig. 3 and S2†). However, the responsible taxa for N-cycling varied with the soil types when subjected to nFe_3O_4@DMSA addition. For example, in LS the decreased proportion of *Anaeromyxobacter*, accompanied by the lower NH_4-N content, was found in the nFe_3O_4@DMSA treatment. *Anaeromyxobacter* is a common resident in paddy soil, and is closely correlated with the process of Fe^{3+} reduction.[53] In general, the N-fixing activity of *Anaeromyxobacter* could be enhanced when ferric iron oxide serves as an electron acceptor for respiration of the iron-reducing bacteria in paddy soil.[54] However, when the ferric iron oxide is downsized to the nano-scale, the negative zeta potential of the particles allows them to percolate through the cell wall of *Anaeromyxobacter* and eventually decrease their proportion.[8] It appeared that in LS the impact of nFe_3O_4@DMSA was more profound than that of nFe_3O_4 on *Anaeromyxobacter*, due to the modified surface characteristics of the nanoparticles. The toxicity of the nanoparticles to some N-fixation microorganisms has also been observed previously.[55] In WS, *Azospirillum* had a higher relative abundance in the nFe_3O_4@DMSA treatment, together with a higher NH_4-N content. *Azospirillum* is not only a strong iron solubilizer, but also has a nitrogenase activity,[2] which induces more N input into soil and thus mineral N content. In RS, a significantly increased proportion of *Burkholderia–Caballeronia–Paraburkholderia* was detected in nFe_3O_4@DMSA compared to the control. Such a phenomenon might be also attributed to the versatile functions of *Burkholderia–Caballeronia–Paraburkholderia* in both N fixation[56] and C cycling.[13] Together, both the surface characteristics and soil types influenced the soil N cycling, with the consequence resting on their balance.

Conclusions

This is the first study to compare the effects of nFe_3O_4 and nFe_3O_4@DMSA on gas production, element cycling and bacterial community in different soils. The results showed that nFe_3O_4@DMSA substantially increased the CO_2 emission, the NH_4-N content, and the BG, BX, and NAG activities, but decreased the CH_4 production in LS and WS. These phenomena were accompanied by the changes of some functional groups and representative lineages in the soil bacterial community. However, a discrepancy was observed in RS, where nFe_3O_4@DMSA increased the CH_4 production but decreased the CO_2 production, an opposite pattern to the other soils. Different mechanisms were proposed to control the biochemical process, with the dominant controlling factor and the final response being dependent on the nanoparticles and the edaphic properties (*e.g.* bioavailable C and Fe species). Moreover, these results need to be confirmed under natural conditions and to see if the impact of nFe_3O_4@DMSA in soil matrices could be reflective in the same way.

Author contributions

Jiangbing Xu: writing – original draft, data curation and visualization. Yaqian Chen: methodology. Jingyi Luo: methodology. Jiatong Xu: methodology. Guoyi Zhou: experimental guidance. Yingliang Yu: software and validation. Lihong Xue: writing – review & editing. Linzhang Yang: writing – review & editing. Shiying He: funding acquisition, methodology and writing – original draft.

Conflicts of interest

The authors declare that they have no known competing financial interests or personal relationships that could have appeared to influence the work reported in this paper.

Acknowledgements

This work was partly supported by the National Natural Science Foundation of China (grant number 41771295, 42130506). We thank Guangzhou Genedenovo Biotechnology Co., Ltd for assisting in sequencing and bioinformatics analysis.

References

1 J. Xu, X. Luo, Y. Wang and Y. Feng, Evaluation of zinc oxide nanoparticles on lettuce (*Lactuca sativa* L.) growth and soil bacterial community, *Environ. Sci. Pollut. Res.*, 2018, **25**, 6026–6035, DOI: **10.1007/s11356-017-0953-7**.

2 A. Sharma, D. Shankhdhar and S. C. Shankhdhar, Enhancing grain iron content of rice by the application of plant growth promoting rhizobacteria, *Plant, Soil Environ.*, 2013, **59**, 89–94.

3 J. Zhang and Y. Lu, Conductive Fe_3O_4 nanoparticles accelerate syntrophic methane production from butyrate oxidation in two different lake sediments, *Front. Microbiol.*, 2016, **7**, 1316, DOI: **10.3389/fmicb.2016.01316**.

4 C. Qiu, Y. Feng, M. Wu, J. Zhang, X. Chen and Z. Li, NanoFe_3O_4 accelerates methanogenic straw degradation in paddy soil enrichments, *Appl. Soil Ecol.*, 2019, **144**, 155–164, DOI: **10.1016/j.apsoil.2019.07.015**.

5 F. Liu, A.-E. Rotaru, P. M. Shrestha, N. S. Malvankar, K. P. Nevin and D. R. Lovley, Magnetite compensates for the lack of a pilin-associated c-type cytochrome in extracellular electron exchange, *Environ. Microbiol.*, 2015, **17**, 648–655, DOI: **10.1111/1462-2920.12485**.

6 G. Yang and J. Wang, Various additives for improving dark fermentative hydrogen production: A review, *Renewable Sustainable Energy Rev.*, 2018, **95**, 130–146, DOI: **10.1016/j.rser.2018.07.029**.

7 D. Zhong, J. Li, W. Ma and F. Qian, Clarifying the synergetic effect of magnetite nanoparticles in the methane production process, *Environ. Sci. Pollut. Res.*, 2020, **27**, 17054–17062, DOI: **10.1007/s11356-020-07828-y**.

8 M. I. Rashid, T. Shahzad, M. Shahid, M. Imran, J. Dhavamani, I. M. Ismail, J. M. Basahi and T. Almeelbi, Toxicity of iron oxide nanoparticles to grass litter decomposition in a sandy soil, *Sci. Rep.*, 2017, **7**, 41965, DOI: **10.1038/srep41965**.

9 Y. S. Perea Vélez, R. Carrillo-González and M. D. C. A. González-Chávez, Interaction of metal nanoparticles–plants–microorganisms in agriculture and soil remediation, *J. Nanopart. Res.*, 2021, **23**, 206, DOI: **10.1007/s11051-021-05269-3**.

10 Q. Tian, X. Wang, F. Mao and X. Guo, Absorption performance of DMSA modified Fe_3O_4@SiO_2 core/shell magnetic nanocomposite for Pb^{2+} removal, *J. Cent. South Univ.*, 2018, **25**, 709–718, DOI: **10.1007/s11771-018-3775-y**.

11 M. Al-Sid-Cheikh, M. Pedrot, A. Dia, M. Davranche, L. Jeanneau, P. Petitjean, M. Bouhnik-Le Coz, M.-A. Cormier and F. Grasset, Trace element and organic matter mobility impacted by Fe_3O_4-nanoparticle surface coating within wetland soil, *Environ. Sci.: Nano*, 2019, **6**, 3049–3059, DOI: **10.1039/C9EN00565J**.

12 M. Kamran, H. Ali, M. F. Saeed, H. F. Bakhat, Z. Hassan, M. Tahir, G. Abbas, M. A. Naeem, M. I. Rashid and G. M. Shah, Unraveling the toxic effects of iron oxide nanoparticles on nitrogen cycling through manure-soil-plant continuum, *Ecotoxicol. Environ. Saf.*, 2020, **205**, 111099, DOI: **10.1016/j.ecoenv.2020.111099**.

13 W. Zhang, X. Jia, S. Chen, J. Wang, R. Ji and L. Zhao, Response of soil microbial communities to engineered nanomaterials in presence of maize (*Zea mays* L.) plants, *Environ. Pollut.*, 2020, **267**, 115608, DOI: **10.1016/j.envpol.2020.115608**.

14 J. Zhou, H. Zhang, J. Liu, L. Gong, X. Yang, T. Zuo, Y. Zhou, J. Wang, X. You, Q. Jia and L. Wang, Effects of Fe_3O_4 nanoparticles on anaerobic digestion enzymes and microbial community of sludge, *Environ. Technol.*, 2021, DOI: **10.1080/09593330.2021.1963324**.

15 S. Y. He, Y. Z. Feng, H. X. Ren, Y. Zhang, N. Gu and X. G. Lin, The impact of iron oxide magnetic nanoparticles on the soil bacterial community, *J. Soils Sediments*, 2011, **11**, 1408–1417, DOI: **10.1007/s11368-011-0415-7**.

16 S. Y. He, Y. Z. Feng, J. Ni, Y. F. Sun, L. H. Xue, Y. F. Feng, Y. L. Yu, X. G. Lin and L. Z. Yang, Different responses of soil microbial metabolic activity to silver and iron oxide nanoparticles, *Chemosphere*, 2016, **147**, 195–202, DOI: **10.1016/j.chemosphere.2015.12.055**.

17 N. Lubick, Risks of nanotechnology remain uncertain, *Environ. Sci. Technol.*, 2008, **42**, 1821–1824.

18 J. Baumann, J. Koser, D. Arndt and J. Filser, The coating makes the difference: acute effects of iron oxide nanoparticles on *Daphnia magna*, *Sci. Total Environ.*, 2014, **484**, 176–184, DOI: **10.1016/j.scitotenv.2014.03.023**.

19 J. T. Buchman, T. Pho, R. S. Rodriguez, Z. V. Feng and C. L. Haynes, Coating iron oxide nanoparticles with mesoporous silica reduces their interaction and impact on *S. oneidensis* MR-1, *Chemosphere*, 2019, **237**, 124511, DOI: **10.1016/j.chemosphere.2019.124511**.

20 S. Bemowsky, A. Rother, W. Willmann, J. Köser, M. Markiewicz, R. Dringen and S. Stolte, Quantification and biodegradability assessment of meso-2,3-dimercaptosuccinic

acid adsorbed on iron oxide nanoparticles, *Nanoscale Adv.*, 2019, **1**, 3670–3679, DOI: **10.1039/c9na00236g**.

21 Y.-Q. Zhang, R. Dringen, C. Petters, W. Rastedt, J. Köser, J. Filser and S. Stolte, Toxicity of dimercaptosuccinate-coated and un-functionalized magnetic iron oxide nanoparticles towards aquatic organisms, *Environ. Sci.: Nano*, 2016, **3**, 754–767, DOI: **10.1039/c5en00222b**.

22 N. Malhotra, J. S. Lee, R. A. D. Liman, J. M. S. Ruallo, O. B. Villaflores, T. R. Ger and C. D. Hsiao, Potential toxicity of iron oxide magnetic nanoparticles: a review, *Molecules*, 2020, **25**, 3159, DOI: **10.3390/molecules25143159**.

23 T. Ben-Moshe, S. Frenk, I. Dror, D. Minz and B. Berkowitz, Effects of metal oxide nanoparticles on soil properties, *Chemosphere*, 2013, **90**, 640–646, DOI: **10.1016/j.chemosphere.2012.09.018**.

24 C. Colombo, G. Palumbo, J. Z. He, R. Pinton and S. Cesco, Review on iron availability in soil: interaction of Fe minerals, plants, and microbes, *J. Soils Sediments*, 2014, **14**, 538–548, DOI: **10.1007/s11368-013-0814-z**.

25 R. Lu, *Analytical methods for soils and agricultural chemistry (in Chinese)*, China Agricultural Science and Technology Press, Beijing, China, 1999.

26 J. G. Caporaso, C. L. Lauber, W. A. Walters, D. Berg-Lyons, C. A. Lozupone, P. J. Turnbaugh, N. Fierer and R. Knight, Global patterns of 16S rRNA diversity at a depth of millions of sequences per sample, *Proc. Natl. Acad. Sci. U. S. A.*, 2011, **108**, 4516.

27 S. Louca, L. W. Parfrey and M. Doebeli, Decoupling function and taxonomy in the global ocean microbiome, *Science*, 2016, **353**, 1272–1277.

28 R Core Team, *R: A language and environment for statistical computing*, R Foundation for Statistical Computing, Vienna, Austria, 2020.

29 J. Han, L. Shi, Y. Wang, Z. Chen and L. Wu, The regulatory role of endogenous iron on greenhouse gas emissions under intensive nitrogen fertilization in subtropical soils of China, *Environ. Sci. Pollut. Res.*, 2018, **25**, 14511–14520, DOI: **10.1007/s11356-018-1666-2**.

30 G. S. Aguilar-Moreno, E. Navarro-Cerón, A. Velázquez-Hernández, G. Hernández-Eugenio, M. Á. Aguilar-Méndez and T. Espinosa-Solares, Enhancing methane yield of chicken litter in anaerobic digestion using magnetite nanoparticles, *Renewable Energy*, 2020, **147**, 204–213, DOI: **10.1016/j.renene.2019.08.111**.

31 E. E. Bestawy, B. F. El-Shatby and A. S. Eltaweil, Integration between bacterial consortium and magnetite (Fe_3O_4) nanoparticles for the treatment of oily industrial wastewater, *World J. Microbiol. Biotechnol.*, 2020, **36**, 141, DOI: **10.1007/s11274-020-02915-1**.

32 A. Ali, R. B. Mahar, R. A. Soomro and S. T. H. Sherazi, Fe_3O_4 nanoparticles facilitated anaerobic digestion of organic fraction of municipal solid waste for enhancement of methane production, *Energy Sources, Part A*, 2017, **39**, 1815–1822, DOI: **10.1080/15567036.2017.1384866**.

33 L. Fu, T. Song, W. Zhang, J. Zhang and Y. Lu, Stimulatory effect of magnetite nanoparticles on a highly enriched butyrate-oxidizing consortium, *Front. Microbiol.*, 2018, **9**, 1480, DOI: **10.3389/fmicb.2018.01480**.

34 J. Huang, K. Ma, X. Xia, K. Gao and Y. Lu, Biochar and magnetite promote methanogenesis during anaerobic decomposition of rice straw, *Soil Biol. Biochem.*, 2020, **143**, 107740, DOI: **10.1016/j.soilbio.2020.107740**.

35 H. Li, J. Chang, P. Liu, L. Fu, D. Ding and Y. Lu, Direct interspecies electron transfer accelerates syntrophic oxidation of butyrate in paddy soil enrichments, *Environ. Microbiol.*, 2015, **17**, 1533–1547, DOI: **10.1111/1462-2920.12576**.

36 L. Xiao, F. Liu, J. Liu, J. Li, Y. Zhang, J. Yu and O. Wang, Nano-Fe_3O_4 particles accelerating electromethanogenesis on an hour-long timescale in wetland soil, *Environ. Sci.: Nano*, 2018, **5**, 436–445, DOI: **10.1039/C7EN00577F**.

37 S. Cheng, C. Qin, H. Xie, W. Wang, Z. Hu, S. Liang and K. Feng, A new insight on the effects of iron oxides and dissimilated metal-reducing bacteria on CH_4 emissions in constructed wetland matrix systems, *Bioresour. Technol.*, 2021, **320**, 124296, DOI: **10.1016/j.biortech.2020.124296**.

38 S. Kato, K. Hashimoto and K. Watanabe, Methanogenesis facilitated by electric syntrophy via (semi)conductive iron-oxide minerals, *Environ. Microbiol.*, 2012, **14**, 1646–1654, DOI: **10.1111/j.1462-2920.2011.02611.x**.

39 T. Borch, R. Kretzschmar, A. Kappler, P. V. Cappellen, M. Ginder-Vogel, A. Voegelin and K. Campbell, Biogeochemical redox processes and their impact on contaminant dynamics, *Environ. Sci. Technol.*, 2010, **44**, 15–23.

40 J. Lin, F. He, G. Owens and Z. Chen, How do phytogenic iron oxide nanoparticles drive redox reactions to reduce cadmium availability in a flooded paddy soil?, *J. Hazard. Mater.*, 2021, **403**, 123736, DOI: **10.1016/j.jhazmat.2020.123736**.

41 N. Chen, D. Huang, G. Liu, L. Chu, G. Fang, C. Zhu, D. Zhou and J. Gao, Active iron species driven hydroxyl radicals formation in oxygenation of different paddy soils: Implications to polycyclic aromatic hydrocarbons degradation, *Water Res.*, 2021, **203**, 117484, DOI: **10.1016/j.watres.2021.117484**.

42 W. Wang, D. Huang, D. Wang, M. Tan, M. Geng, C. Zhu, N. Chen and D. Zhou, Extensive production of hydroxyl radicals during oxygenation of anoxic paddy soils: Implications to imidacloprid degradation, *Chemosphere*, 2022, **286**, 131565, DOI: **10.1016/j.chemosphere.2021.131565**.

43 S. He, Y. Feng, H. Ren, Y. Zhang, N. Gu and X. Lin, The impact of iron oxide magnetic nanoparticles on the soil bacterial community, *J. Soils Sediments*, 2011, **11**, 1408–1417, DOI: **10.1007/s11368-011-0415-7**.

44 M. C. Marx, M. Wood and S. C. Jarvis, A microplate fluorimetric assay for the study of enzyme diversity in soils, *Soil Biol. Biochem.*, 2001, **33**, 1633–1640.

45 T. T. Awet, Y. Kohl, F. Meier, S. Straskraba, A. L. Gruen, T. Ruf, C. Jost, R. Drexel, E. Tunc and C. Emmerling, Effects of polystyrene nanoparticles on the microbiota and functional diversity of enzymes in soil, *Environ. Sci. Eur.*, 2018, **30**, 11, DOI: **10.1186/s12302-018-0140-6**.

46 J. A. Galhardi, L. F. Fraceto, K. J. Wilkinson and S. Ghoshal, Soil Enzyme Activities as an Integral Part of the Environmental Risk Assessment of Nanopesticides, *J. Agric. Food Chem.*, 2020, **68**, 8514–8516, DOI: **10.1021/acs.jafc.0c04344**.

47 D. P. German, M. N. Weintraub, A. S. Grandy, C. L. Lauber, Z. L. Rinkes and S. D. Allison, Optimization of hydrolytic and oxidative enzyme methods for ecosystem studies, *Soil Biol. Biochem.*, 2011, **43**, 1387–1397, DOI: **10.1016/j.soilbio.2011.03.017**.

48 R. L. Sinsabaugh, C. L. Lauber, M. N. Weintraub, B. Ahmed, S. D. Allison, C. Crenshaw, A. R. Contosta, D. Cusack, S. Frey, M. E. Gallo, T. B. Gartner, S. E. Hobbie, K. Holland, B. L. Keeler, J. S. Powers, M. Stursova, C. Takacs-Vesbach, M. P. Waldrop, M. D. Wallenstein, D. R. Zak and L. H. Zeglin, Stoichiometry of soil enzyme activity at global scale, *Ecol. Lett.*, 2008, **11**, 1252–1264, DOI: **10.1111/j.1461-0248.2008.01245.x**.

49 Y. Xiang, F. Kang, Y. Xiang and Y. Jiao, Effects of humic acid-modified magnetic Fe_3O_4/MgAl-layered double hydroxide on the plant growth, soil enzyme activity, and metal availability, *Ecotoxicol. Environ. Saf.*, 2019, **182**, 109424, DOI: **10.1016/j.ecoenv.2019.109424**.

50 T. You, D. Liu, J. Chen, Z. Yang, R. Dou, X. Gao and L. Wang, Effects of metal oxide nanoparticles on soil enzyme activities and bacterial communities in two different soil types, *J. Soils Sediments*, 2018, **18**, 211–221, DOI: **10.1007/s11368-017-1716-2**.

51 D. M. Zhou, S. Y. Jin, Y. J. Wang, P. Wang, N. Y. Weng and Y. Wang, Assessing the impact of iron-based nanoparticles on pH, dissolved organic carbon, and nutrient availability in soils, *Soil Sediment Contam.*, 2012, **21**, 101–114, DOI: **10.1080/15320383.2012.636778**.

52 H. W. Scherer and Y. Zhang, Studies on the mechanisms of fixation and release of ammonium in paddy soils after flooding. I. Effect of iron oxides on ammonium fixation, *J. Plant Nutr. Soil Sci.*, 1999, **162**, 593–597.

53 K. Wang, R. Jia, L. Li, R. Jiang and D. Qu, Community structure of *Anaeromyxobacter* in Fe(III) reducing enriched cultures of paddy soils, *J. Soils Sediments*, 2020, **20**, 1621–1631, DOI: **10.1007/s11368-019-02529-7**.

54 Y. Masuda, Y. Shiratori, H. Ohba, T. Ishida, R. Takano, S. Satoh, W. Shen, N. Gao, H. Itoh and K. Senoo, Enhancement of the nitrogen-fixing activity of paddy soils owing to iron application, *Soil Sci. Plant Nutr.*, 2021, **67**, 243–247.

55 K. Jiao, B. Yang, H. Wang, W. Xu, C. Zhang, Y. Gao, W. Sun, F. Li and D. Ji, The individual and combined effects of polystyrene and silver nanoparticles on nitrogen transformation and bacterial communities in an agricultural soil, *Sci. Total Environ.*, 2022, **820**, 153358, DOI: **10.1016/j.scitotenv.2022.153358**.

56 M. Kumar, R. S. Tomar, H. Lade and D. Paul, Methylotrophic bacteria in sustainable agriculture, *World J. Microbiol. Biotechnol.*, 2016, **32**, 120, DOI: **10.1007/s11274-016-2074-8**.

